Am J Cancer Res 2019;9(5):927-944
www.ajcr.us /ISSN:2156-6976/ajcr0091847

Original Article

The miR-873/NDFIP1 axis promotes hepatocellular carcinoma growth and metastasis through the AKT/mTOR-mediated Warburg effect

Yuyu Zhang[1], Chengbin Zhang[2], Qin Zhao[3], Wei Wei[1], Zhuo Dong[1], Lihong Shao[3], Jianbo Li[4], Wei Wu[5], Heng Zhang[4], He Huang[4,6], Feng Liu[7], Shunzi Jin[1]

[1]NHC Key Laboratory of Radiobiology, Jilin University, Changchun, China; Departments of [2]Pathology, [3]Radiation Oncology, The First Bethune Hospital of Jilin University, Changchun, China; [4]Department of Histology and Embryology, Xiang Ya School of Medicine, Central South University, Changsha, Hunan, China; [5]Department of General Surgery, Xiangya Hospital, Central South University, Changsha, Hunan, China; [6]State Key Laboratory of Pathogenesis, Prevention and Treatment of High Incidence Diseases in Central Asia, School of Preclinical Medicine, Xinjiang Medical University, Urumqi, Xinjiang, China; [7]Department of Nephrology, China-Japan Union Hospital of Jilin University, Changchun, China

Received January 25, 2019; Accepted April 4, 2019; Epub May 1, 2019; Published May 15, 2019

Abstract: Hepatocellular carcinoma (HCC) progression depends on cellular metabolic reprogramming as both direct and indirect consequence of oncogenic lesions. However, the underlying mechanisms are still understood poorly. Here, we report that miR-873 promotes Warburg effect in HCC cells by increasing glucose uptake, extracellular acidification rate (ECAR), lactate production, and ATP generation, and decreasing oxygen consumption rate (OCR) in HCC cells. Mechanistically, we show that miR-873 activates the key glycolytic proteins AKT/mTOR via targeting NDFIP1 which triggers metabolic shift. We further demonstrate that enhanced glycolysis is essential for the role of miR-873 to drive HCC progression. By using immunohistochemistry analysis, we show a link between the aberrant expression of miR-873, NDFIP1, and phospho-AKT in clinical HCC samples. We also found that miR-873 was up-regulated by HIF1α, a critical glycolysis-related transcription factor. However, BAY 87-2243, a HIF1α specific inhibitor, blocks miR-873 mediated tumor growth and metastasis in nude mice. Collectively, our data uncover a previously unappreciated function of miR-873 in HCC cell metabolism and tumorigenesis, suggesting that targeting miR-873/NDFIP1 axis could be a potential therapeutic strategy for the treatment of HCC patients.

Keywords: miR-873, NDFIP1, HCC, Warburg effect

Introduction

Hepatocellular carcinoma (HCC) is the third most common cause of cancer-related death, and its incidence is expected to increase worldwide [1]. As an inherent feature of solid tumors, including HCC, hypoxia or inadequate oxygen supply contributes to the metabolic reprogramming of cancer cells [2]. Tumor cells modify their metabolism to adapt to challenging hypoxic environments to facilitate continuous growth. This phenomenon is referred to as the Warburg effect and is a core metabolic hallmark of cancer [3]. In addition to generating ATP, this metabolic reprogramming provides glycolytic intermediates that are needed to address the biosynthetic needs of fast-growing tumors [4]. Thus, targeting glycolysis in HCC cells, especially in hypoxic environments, is likely to be of great value for the treatment of HCC.

MicroRNAs (miRNAs) are 18- to 22-nucleotide-long noncoding RNAs [5]. They regulate gene expression at the post-transcriptional level by binding to the 3'-untranslated regions (UTRs) of their target genes to either block mRNA translation or trigger mRNA degradation [6]. It is becoming increasingly evident that miRNAs are key modulators of the initiation and progression of HCC [7]. MiRNAs can act as oncogenes or tumor suppressors depending on their targets [8]. Recently, a series of miRNAs were found to

be involved in the regulation of glucose metabolism and hypoxia in cancer [9]. For example, miR-186, miR-199a-5p, and miR-122 have been shown to control the Warburg effect in HCC [10]. Notably, miR-873 was shown to be ectopically expressed in different cancers, such as glioblastoma multiforme, lung adenocarcinoma, and ovarian cancer. By targeting SRCIN1, CDK3, IGF2BP1, ABCB1, and TRIM25, miR-873 regulates the growth and metastasis of different types of cancer [11-14]. However, controversial roles of miR-873 were observed and it is unknown whether it regulates glucose metabolism or contributes to hepatocarcinogenesis.

In this study, we show that miR-873 is a novel oncomiR in HCC. By directly targeting Nedd4 family-interacting protein 1 (NDFIP1), miR-873 promoted glycolysis to drive the progression of HCC. Importantly, in patients with HCC, the abundance of miR-873 was negatively correlated with NDFIP1 expression.

Methods

Cell culture, reagents, and plasmids

Human HCC and normal liver cell lines were obtained from Cell Bank of Chinese Academy of Science (Peking). All of these cells were cultured in RPMI-1640 medium supplemented with 10% fetal bovine serum (Gibco), 100 μg/ml streptomycin, and 100 IU/ml penicillin at 37°C in a humidified incubator with 5% CO_2. The primary antibodies against DNFIP1, p-Akt, Akt, p-S6K1, β-actin, GAPDH were purchased from Cell Signal Technology (Beverly, USA). To generate lentiviral constructs, miR-873 (Gene ID: 100126316) and NDFIP1 genes were separately generated by PCR amplification and the PCR products were then cloned into pCDH-CMV (System Biosciences, USA). miRNA mimics and negative control of miRNA mimics (NC) were synthesized by GenePharma with the following sequences: miR-873 mimics, 5'-GCA GGA ACU UGU GAG UCU CCU-3'; NC mimics, 5'-UUG UAC UAC ACA AAA GUA CUG-3'. The inhibitors of miR-873 and control oligonucleotides was obtained from Exiqon. siNDFIP1-#1: 5'-UUUGGUCUCUCUCUAAUUA-3'; siNDFIP1-#2: 5'-CCUCCACCAUAUAGUAGUA-3'. siHIF1a-#1: 5'-CUGAUGACCAGCAACUUGA-3'; siHIF1a-#2: 5'-AAGCAUUUCUCUCAUUUCCUCAUGG-3'. Mitomycin-C (Sigma-Aldrich, M4287), Z-VAD (Sigma-Aldrich, V116).

RNA extraction and quantitative real-time RT-PCR (qRT-PCR)

The cells and tissues were collected and washed with ice-cold PBS. Subsequently, 1 ml of TRIzol reagent was added. Total RNA was extracted using a miRNA isolation kit (Takara). Then reverse transcription was performed using one step PrimeScript® miRNA cDNA synthesis kit (Takara) following the manufacturer's instructions. U6 small nuclear RNA acted as an internal control, and its sequence-specific primers were: forward, 5'-GCTCTCGCATCGCAGCA-3', reverse, 5'-CTCGGCTAGCGCTACTC-3'; GAPDH forward 5'-GGAGCCAAAAGGGTCATC-3', and reverse 5'-CCAGTGAGTTTCCCGTTC-3'. The amplification of PCR was performed using the SYBR Premix Ex Taq (Takara) on a LightCycler® (Roche Diagnostics). The condition of PCR was as follows: 30 s at 94°C, 40 cycles at 95°C, 5 s, and 60°C for 20 s. The relative expression levels were calculated by using the comparative $2^{-\Delta CT}$ method. The expression of miR-873 in clinical samples was detected by real-time RT-PCR, and the mean value of miR-873 expression was calculated. The samples that had miR-873 expression equal to or greater than mean value were divided into high miR-873 expression group. The samples that had miR-873 expression lower than mean value were divided into low miR-873 expression group.

Western blotting

Briefly, lysates from cultured cells or tissues were prepared in modified RIPA buffer (150 mM 150 mM sodium chloride, 50 mM Tris-HCl [pH 7.4], 1% Triton, 0.5% sodium deoxycholate, 0.1% SDS) plus 25 μg/ml leupeptin, 10 μg/ml aprotinin. The protein concentrations were determined by using a BCA Protein Assay Reagent kit (Pierce Biotechnology, USA). Then cell or tissue protein extracts were separated using SDS polyacrylamide gel electrophoresis and transferred to a PVDF membrane (Millipore, MA). The membranes were incubated with indicated antibody for overnight at 4°C. After primary antibody incubation, PVDF membranes were washed three times for 30 min in TBST buffer (0.1% Tween in PBS) before incubation in the appropriate horseradish peroxidase-linked secondary antibody for 1 hour at room temperature. Finally, membranes were washed three times, and immunoreactive proteins were assayed using an enhanced chemiluminescence substrate reaction (Thermo Scientific,

USA) according to the manufacturer's instructions. Image Lab analysis software (BioRad, USA) was used for quantification of bands intensities and statistical analysis. Bands intensities were expressed as a ratio between target proteins and their corresponding GAPDH. Then the ratio value was normalized to controls. Experiments were repeated at least three times. The data were expressed as mean ± SD.

Cell growth, migration and invasion assays

Cell growth was examined with a Cell Counting Kit (CCK)-8 Kit according to the manufacturer's instructions (Dojindo). Cells were plated in 96-well plates at a density of 5000 cells per well, and pre-incubated. At designed time points (6, 12, 24, 48 and 72 hours) post culture, 10 μL of CCK-8 solution was added to each well. And the cells were further cultured for 2 hours. Absorbance was read at 450 nm using a microplate reader.

Cell invasion assay was performed with Matrigel Invasion Chambers following the manufacturer's instructions (BD Biosciences). Briefly, transfected cells were placed on the upper surface of the transwell insert. After 16 h, the invasive cells were fixed with 4% paraformaldehyde and stained with 0.5% crystal violet. The number of invasive cells was averaged in five randomly selected microscope visions and photographed.

Metabolism measurements

Glucose Uptake Colorimetric Assay kit, Lactate Assay Kit II, ATP Colorimetric Assay kit, and Lactate Dehydrogenase Activity Assay Kit were used to determine glucose uptake, lactate and ATP production, and activities of LDH (L-lactate dehydrogenase), respectively, according to the manufacturer's protocols (Biovision). For glucose uptake colorimetric assay, cells were seeded at a density of 1500 cells per well in a 96-well plate. The cells were starved for glucose for 40 min by preincubating with 100 μl Krebs-Ringer-Phosphate-HEPES (KRPH) buffer containing 2% BSA. Ten microliters of 10 mM 2-DG (2-deoxyglucose) were added and the cells incubated for 20 min. For lactate and ATP assays, 1×10^6 cells were homogenized in 100 μl corresponding assay buffer provided by the kits. Samples were centrifuged, and the soluble fraction was assayed. For lactate dehydrogenase activity analysis, 1×10^6 cells were lysed in 100 μl assay buffer in the kit and centrifuged at 10,000 × g for 15 min at 4°C. Thirty microliters of supernatants were added to a 96-well plate.

The extracellular acidification rate (ECAR) and cellular oxygen consumption rate (OCR) were determined using the Seahorse XF^e 96 Extracellular Flux Analyzer (Seahorse Bioscience). Following the manufacturer's protocols, all experiments were carried out. ECAR and OCR were examined using Seahorse XF Glycolysis Stress Test Kit and Seahorse XF Cell Mito Stress Test Kit, respectively. Briefly, 2×10^4 cells/well were seeded into a Seahorse XF 96 cell culture microplate. After baseline measurements, for ECAR, glucose, the oxidative phosphorylation inhibitor oligomycin, and the glycolytic inhibitor 2-DG were sequentially injected into each well at indicated time points. For OCR, oligomycin, the reversible inhibitor of oxidative phosphorylation FCCP (p-trifluoromethoxy carbonyl cyanide phenylhydrazone), and the mitochondrial complex I inhibitor rotenone plus the mitochondrial complex III inhibitor antimycin A (Rote/AA) were sequentially injected. The Seahorse XF-96 Wave software was used to analyze the data. OCR is shown in pmols/minute and ECAR in mpH/minute. For basal oxygen consumption rate measurement, 500 million trypsinized cells were suspended in culture medium in a 0.5 ml volume and measured by an Oxytherm unit (Strathkelvin Instrument Ltd.). All values were normalized to protein concentration.

Gas chromatography-mass spectrometry (GC-MS) analysis of metabolites

HCC cells overexpressing indicated plasmids were incubated in the culture medium without glucose and FBS for 7 h, followed by supplement with 10% FBS and 25 mM of ^{13}C-labeled glucose (Cambridge isotope laboratory) and continued culture for 36 h. Metabolites were extracted from cells as previously described. Briefly, cells were rinsed with cold PBS and lysed in cold 50% acetonitrile, with three quick cycles of freeze-thawing using liquid nitrogen and 37°C water bath. Then, the lysates were centrifuged, and the supernatant was dried in termovap nitrogen sample concentrator and resuspended in 80% CH_3OH/H_2O with ribitol (0.2 mg/ml), followed by sonication and cen-

trifugation. The supernatant was dried again and then derivatized for GC-MS analysis. Data were collected on an Agilent 6890N GC × GC-TOF-MS, a two-dimensional gas chromatography time-of-flight MS coupled with a Pegasus HT time-of-flight MS (Leco Corporation).

Intracellular ROS measurement

Trypsinized cells were stained with 2 μM of CellROX DeepRed (Life Technologies) in PBS containing 5% FBS at 37°C for 30 min. Intracellular ROS production was analyzed by FACSVerse flow cytometer (BD Bioscience). Gain and amplifier settings were held constant during the experiment.

Transfection and luciferase assay

Renilla reporter pRL-TK and pGL2-promoter empty vector were cotransfected with or without indicated vector into HEK293 cells. Forty-eight hours after transfection, cells were lysed, and luciferase activity was assessed using the dual-luciferase reporter assay system (Promega). All experiments were repeated at least four times.

Tumor xenograft study

In brief, Hep3B cells (5×10^5 cells per mouse in 10 μL total) were injected into four-week-old male BALB/c-nude mice (n = 5 per group). When tumors reached about 50 mm^3, BAY 87-2243 was used to treat the mice for 15 days. Then tumors were collected and measured by bioluminescence with an IVIS Lumina Imaging System (Xenogen). These procedures were carried out following approval by the Institutional Animal Care and Use Committee.

Tissue samples and ethics statement

All of the HCC tissues were obtained from patients collected at Jilin University Affiliated Hospital. The normal tissue samples were collected from adjacent tissues that were not more than 3 cm away from the tumors. The tumor samples were further confirmed by pathologists and classified according to World Health Organization classification. This study was approved by the Ethical Committee of Jilin University Hospital (Protocol Number: 20160322). The written informed consent was obtained from every participant who involved in this study.

Statistical analysis

All of the experiments in vitro were performed in triplicate and repeated 3 times. Statistical analysis was performed using two-tailed Student's t-test. The statistical assays were calculated by the SPSS 17.0 statistical software package. The correlation between the expression of miR-873 and NDFIP1 was examined by Spearman rank analysis using GraphPad Prism 7. *P* values of less than 0.05 were considered statistically significant. $*P < 0.05$; $**P < 0.01$.

Results

MiR-873 is increased in HCC and associated with poor prognosis

The expression pattern of miR-873 was evaluated using qRT-PCR to investigate its potential role in HCC. In a cohort of 86 patients with HCC, the relative expression of miR-873 was significantly increased in HCC tumor tissues compared with non-tumor tissues (**Figure 1A**). In addition, miR-873 levels were higher in advanced HCC compared with localized HCC, suggesting that miR-873 could be related to the aggressiveness and poor prognosis of HCC (**Figure 1B** and **Table 1**). Moreover, miR-873 expression was positively associated with tumor, node, metastasis stage and metastasis, but was negatively correlated with tumor differentiation (**Table 1**). As expected, Kaplan-Meier analysis indicated that HCC patients with low levels of miR-873 expression had a much longer overall survival and time to relapse than those with high levels (**Figure 1C** and **1D**). Multivariate analysis revealed that tumor stage and miR-873 expression were independent predictors of overall survival (**Table 2**). Detailed clinical information regarding the HCC samples is shown in **Tables 3** and **4**. Furthermore, compared with HCC cell lines (SMMC-7721, HepG2, Hep3B, SK-HEP-1, and MHCC97H), immortalized human liver epithelial cell lines (L02, 7701, and 7702) showed relatively low miR-873 expression (**Figure 1E**). Therefore, miR-873 might be an oncomiR and an important prognostic marker in HCC.

MiR-873 promotes the proliferation, migration, and invasion of HCC cells

Since miR-873 was upregulated in HCC, we evaluated its biological effects on tumorigene-

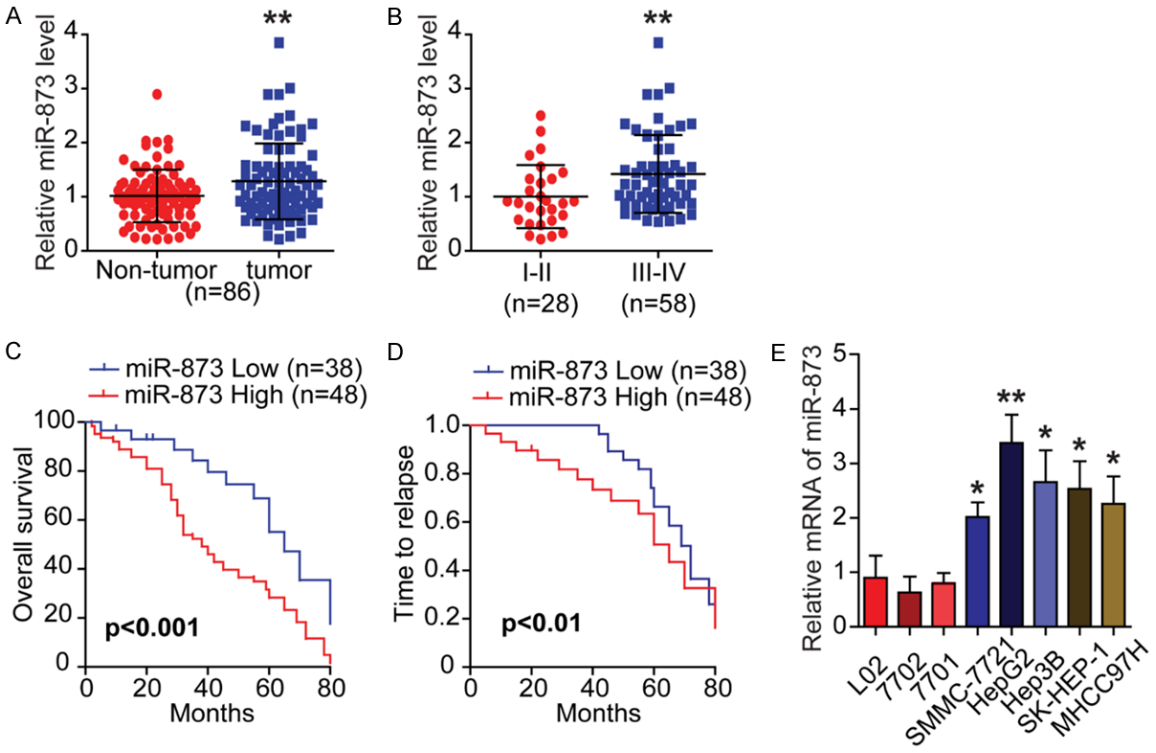

Figure 1. MiR-873 is upregulated in HCC and associated with poor prognosis. A. Scatter dot plots illustrate that the expression of miR-873 is significantly increased in tumor tissues compared with non-tumor ones in a cohort of HCC specimens (n = 86). B. The expression of miR-873 is higher in advanced HCC compared with localized ones. C and D. Kaplan-Meier analysis indicates that the HCC patients with low levels of miR-873 have a much longer time to relapse (TTR) or overall survival (OS). E. qRT-PCR shows the relative expression of miR-873 in HCC cell lines (SMMC-7721, HepG2, Hep3B, SK-HEP-1, and MHCC97H) and the immortalized human liver epithelial cell lines (L02, 7701, and 7702). All data are from three independent experiments. *$P < 0.05$ and **$P < 0.01$.

sis. We transfected miR-873 mimics into SMMC-7721 cells, which express miR-873 at a low level compared to the other HCC cell lines, to investigate the role of miR-873 (**Figure 2A**). CCK-8 analysis showed that miR-873 overexpression significantly promoted cell proliferation (**Figure 2B**). Moreover, miR-873 overexpression significantly increased cell migration and invasion in SMMC-7721 cells with (**Figure 2C** and **2D**) or without (Figure S1) mitomycin C treatment. In contrast, silencing miR-873 inhibited the proliferation, migration, and invasion of Hep3B cells (**Figure 2E-H**), suggesting that silencing miR-873 could inhibit the proliferative and metastatic potential of HCC cells.

MiR-873 promotes the Warburg effect in HCC cells

Since glycolysis promotes the progression of HCC [2], we examined whether miR-873 has a role in glycolysis in HCC cells. To this end, the ECAR was measured initially. A significant reduction in both the basal and maximal ECAR in Hep3B cells with miR-873 silencing was observed (**Figure 3A**, left panel). We also found that silencing miR-873 decreased glucose uptake (**Figure 3B**) and lactate production (**Figure 3C**), accompanied by increased oxygen consumption (**Figure 3A**, right-panel, and **Figure 3D**). This is further confirmed by another anti-miR-873 sequence (Figure S2A-D). Conversely, miR-873 overexpression significantly increased the ECAR, glucose uptake, and lactate production in SMMC-7721 cells, accompanied by decreased oxygen consumption (**Figure 3E-G**). Similar results were observed in SKHEP-1 cells (data not shown). Our results suggest that miR-873 expression facilitates glycolytic metabolism in HCC cells.

To further confirm the critical role of miR-873 in regulating the Warburg effect in HCC cells, we traced the metabolic flux of ^{13}C-labeled glucose in SMMC-7721 cells with miR-873 overexpression using gas chromatography-mass spe-

Table 1. Relationship between miR-873 expression and clinicopathological features of HCC patients (n = 86)

Variable	Relative miR-873 expression		*P*-value
	Low (n = 38)	High (n = 48)	
Age			NS
≤ 50	18	29	
> 50	20	19	
Gender			NS
Male	25	37	
Female	13	11	
Histological differentiation			P < 0.05
I-II	15	30	
III-IV	23	18	
Tumor size			P < 0.05
≤ 5 cm	24	20	
> 5 cm	14	28	
Distant metastasis			P < 0.05
Yes	15	32	
No	23	16	
Tumor stage			P < 0.01
I-II	19	9	
III-IV	19	39	
Intrahepatic metastasis			NS
Yes	22	23	
No	13	25	
AFP (μg/L)			NS
≤ 20	17	21	
> 20	21	27	
Liver Cirrhosis			NS
Yes	27	33	
No	11	15	

Note: HCC patients were divided into miR-873 high group and low group according to the analysis of qRT-PCR detection. NS, not significant between different group; AFP, alpha-fetoprotein. Differences among variables were evaluated by x^2 or Fisher's exact x^2-test.

ctrometry. It was found that the level of ^{13}C-labeled glucose was significantly decreased in the culture medium of SMMC-7721 cells with miR-873 overexpression (**Figure 3H**), suggesting enhanced glucose uptake from the medium by these cells. Consistently, we observed elevated levels of ^{13}C-labeled glucose-6-phosphate (G6P), 1,6-bisphosphate (F1,6BP), and phosphoenolpyruvate (PEP) in miR-873-overexpressing SMMC-7721 cells (Figure S2E-G). However, the level of ^{13}C-labeled pyruvate was not significantly different between miR-873-overexpressing cells and control cells (Figure S2H). MiR-873 overexpression also enhanced the levels of ^{13}C-labeled intracellular and extracellular lactate (**Figure 3I**), confirming that miR-873 promoted glycolysis in HCC cells. However, miR-873 overexpression significantly decreased the levels of TCA cycle metabolites, including citrate, succinate, fumarate, and malate (Figure S2I), suggesting that miR-873 inhibited the oxidative phosphorylation of glucose in HCC cells. Collectively, our findings reveal that miR-873 drives glycolytic metabolism rather than oxidative phosphorylation in HCC cells.

MiR-873 inhibits NDFIP1 expression by targeting its 3'-UTR

To elucidate the mechanism underlying the effect of miR-873 in HCC, we used three different mRNA target-prediction algorithms (TargetScan, miRanda, and TargetRank) to identify potential direct targets of miR-873 based on binding sites in the 3'-UTRs of candidate genes that were associated with glycolysis. On the basis of these mRNA target-prediction algorithms, we identified NDFIP1 as a potential target of miR-873 (**Figure 4A**). We chose NDFIP1 as a candidate target gene because it was shown to regulate the PTEN/AKT signaling pathway [15]. To confirm this *in silico* prediction, we cloned the 3'-UTR of NDFIP1 containing the miR-873 target site into a *Renilla* luciferase reporter construct (**Figure 4B**) and established a luciferase reporter assay with precursor miR-873 (pre-miR-873) transfected into HEK293T cells. We observed a significant reduction in the luciferase activity of the reporter construct containing the NDFIP1 3'-UTR in the presence of miR-873, while miR-873 did not change the luciferase activity of the mutant 3'-UTR (**Figure 4C**). To further confirm that NDFIP1 is a target for miR-873, we examined the level of endogenous NDFIP1 protein after transiently transfecting HEK293T cells with pre-miR-873. As shown in **Figure 4D**, the level of NDFIP1 expression decreased as the concentration of transfected pre-miR-873 was increased. The correlation between miR-873 and NDFIP1 expres-

Table 2. Univariate and multivariate analysis of factors associated with survival in HCC patients (n = 86)

Variable	Univariate analysis		Multivariate analysis	
	HR (95% CI)	*P*-value	HR (95% CI)	*P*-value
Gender				
Male vs. Female	0.942 (0.571-1.555)	0.816		
Age				
≤ 50 vs. > 50	0.917 (0.586-1.433)	0.702		
Histological differentiation				
I-II vs. III-IV	1.859 (1.183-2.919)	0.007		
Tumor size				
≤ 5 cm vs. > 5 cm	1.564 (0.996-2.455)	0.052		
Distant metastasis				
Yes vs. No	1.079 (1.067-2.641)	0.025		
Tumor stage				
I-II vs. III-IV	2.321 (1.384-3.893)	0.001	1.823 (1.039-3.201)	0.036
Liver cirrhosis				
Yes vs. No	1.135 (0.701-1.837)	0.607		
AFP (μg/L)				
≤ 20 vs. >20	0.875 (0.559-1.369)	0.558		
miR-873 expression				
High vs. Low	2.189 (1.368-2.488)	0.001	1.757 (1.061-2.912)	0.029

sion in 20 paired clinical HCC samples was also investigated using qRT-PCR. As expected, miR-873 expression was inversely correlated with the levels of NDFIP1 mRNA in the 20 paired HCC samples (r = -0.62, **Figure 4E**). The level of NDFIP1 mRNA was found to be lower in HCC tissues than in corresponding non-HCC tissues (**Figure 4F**). In addition, immunohistochemical staining showed that miR-873 expression was significantly lower in HCC tissues with high NDFIP1 expression than in those with low NDFIP1 expression, further suggesting an inverse relationship between the expression of miR-873 and NDFIP1 (**Figure 4G**). As expected, we further confirmed that miR-873 promoted glycolysis by inhibiting NDFIP1, since overexpression of NDFIP1 could reverse the enhanced glycolysis induced by miR-873 (Figure S3).

MiR-873 promotes the proliferation, migration, and invasion of HCC cells via NDFIP1

To investigate whether miR-873 promotes HCC tumorigenesis by silencing NDFIP1, we assessed the role of NDFIP1 on HCC cell proliferation, migration, and invasion using gain-and-loss assays. We observed that NDFIP1 overexpression inhibited cell proliferation, migration, and invasion in the presence or absence of the apoptosis inhibitor Z-VAD (Figure S4). Moreover, we found that the simultaneous inhibition of NDFIP1 and miR-873 expression in Hep3B cells restored their proliferation and metastatic capacity (**Figures 5A-D** and S5A-D), while the simultaneous overexpression of NDFIP1 and miR-873 in SMMC-7721 cells eliminated the role of miR-873 in proliferation and metastasis (**Figure 5E-G**). We also found that overexpression of NDFP1 can reverse miR-873-induced cell proliferation and invasion effect (Figure S5E-G). These results indicate that miR-873 may promote proliferation, migration, and invasion via NDFIP1.

Phosphorylated AKT is required for the metabolic shift induced by miR-873

Next, we aimed to identify the target proteins located downstream of the miR-873/NDFIP1 axis. Previous reports have demonstrated that hypoxia-inducible factor (HIF) and c-Myc play central roles in regulating cell glycolysis [2, 8]. However, immunoblot analysis revealed no difference in the expression of HIF1α and c-Myc protein between miR-873-overexpressing HCC cells and control cells (**Figure 6A**). Given that NDFIP1 expression decreases AKT/mammalian target of rapamycin (mTOR) signaling in cancer

Table 3. HCC samples clinical information (Part I)

Sample ID	Age	Gender	Histological differentiation	Tumor size	Distant metastasis	Tumor stage	Intrahepatic metastasis	AFP	Liver cirrhosis
1	47	F	I	5.1	Yes	IV	Yes	14.32	No
2	50	M	III	2.5	No	I	No	6.32	No
3	41	F	II	4.6	No	II	Yes	11.24	No
4	40	M	III	4.4	No	II	Yes	3.48	No
5	44	M	II	3.1	No	II	No	9.45	Yes
6	59	F	II	2.2	No	III	No	8.74	Yes
7	60	M	I	4.3	Yes	IV	No	19.15	No
8	58	F	III	10.6	Yes	IV	No	448.65	Yes
9	77	M	III	1.9	No	II	No	2.48	Yes
10	84	M	IV	3.5	No	I	Yes	117.28	No
11	77	M	II	2.7	No	II	No	6.63	Yes
12	69	M	I	1.4	No	II	Yes	6.61	No
13	70	M	III	3.4	Yes	IV	No	15.32	Yes
14	41	F	I	9.8	Yes	IV	Yes	14.52	Yes
15	46	M	IV	2.1	No	II	No	6.26	Yes
16	79	F	II	8.9	Yes	IV	No	58.36	No
17	68	M	IV	7.8	Yes	IV	Yes	482.35	Yes
18	50	M	III	3.2	No	I	No	14.37	No
19	48	M	II	2.5	No	II	No	388.14	No
20	47	M	III	6.5	Yes	IV	Yes	94.26	Yes
21	38	F	III	1.5	No	I	No	14.26	No
22	87	M	IV	11.6	Yes	IV	Yes	554.24	Yes
23	56	F	II	5.6	Yes	IV	No	89.26	Yes
24	76	M	II	11.7	Yes	IV	Yes	392.63	Yes
25	74	M	IV	7	Yes	IV	No	518.24	Yes
26	81	M	II	6.1	Yes	IV	No	12.44	Yes
27	46	M	III	3.8	No	I	No	6.89	Yes
28	47	M	I	6.6	Yes	IV	Yes	29.37	Yes
29	54	M	II	10.2	Yes	IV	Yes	898.47	Yes
30	80	M	III	9.5	Yes	IV	No	449.25	Yes
31	41	M	III	4.3	Yes	IV	Yes	848.23	Yes
32	47	M	II	11.9	Yes	IV	Yes	662.15	Yes
33	37	F	IV	3.9	Yes	IV	No	15.45	Yes
34	55	M	II	2.7	Yes	IV	No	11.47	Yes
35	81	M	IV	6.7	No	III	Yes	512.24	No
36	39	M	I	4.9	Yes	IV	Yes	42.26	Yes
37	42	F	III	4.4	No	III	No	228.3	Yes
38	48	M	I	1.6	No	II	No	16.41	Yes
39	50	M	I	11.8	Yes	IV	Yes	752.63	Yes
40	39	M	IV	12.8	Yes	IV	Yes	479.22	Yes
41	85	M	I	14.8	Yes	IV	Yes	632.29	Yes
42	36	M	IV	2.9	No	III	No	3.21	Yes
43	48	M	I	2.7	No	II	No	2.84	Yes

cells and AKT/mTOR activation renders tumor cells dependent on aerobic glycolysis for their continued growth and survival, we hypothesized that miR-873 might stimulate HCC cell

Table 4. HCC samples clinical information (Part II)

Sample ID	Age	Gender	Histological differentiation	Tumor size	Distant metastasis	Tumor stage	Intrahepatic metastasis	AFP	Liver cirrhosis
44	72	M	IV	7.7	Yes	IV	Yes	521.38	Yes
45	39	M	I	9	Yes	IV	Yes	87.26	Yes
46	49	M	I	12.7	Yes	IV	Yes	295.44	No
47	40	F	I	4.7	No	II	Yes	18.48	Yes
48	50	M	II	1.2	No	II	No	15.61	Yes
49	64	F	III	3.4	No	II	No	52.15	Yes
50	63	M	II	7.6	Yes	IV	Yes	17.46	Yes
51	42	M	I	3.8	No	III	Yes	6.63	No
52	44	M	I	7.6	Yes	IV	Yes	669.26	Yes
53	47	F	II	2.5	No	II	No	13.26	Yes
54	64	F	I	5.4	No	III	No	112.39	No
55	82	M	IV	11	No	I	No	18.31	Yes
56	45	F	II	13.6	Yes	IV	Yes	892.48	Yes
57	75	F	IV	3.9	Yes	IV	Yes	526.3	No
58	56	M	II	8.7	Yes	IV	Yes	924.52	Yes
59	45	M	I	8.4	Yes	IV	Yes	965.52	No
60	41	M	III	10.4	Yes	IV	Yes	654.48	Yes
61	66	M	II	6.2	No	III	Yes	329.64	Yes
62	49	M	II	4.9	Yes	IV	Yes	14.12	Yes
63	73	M	III	2.9	No	I	No	18.26	Yes
64	46	F	IV	3.4	No	I	No	7.35	No
65	39	M	III	4.5	Yes	IV	No	328.44	Yes
66	79	F	IV	4.8	No	III	Yes	188.4	No
67	59	M	II	2.8	No	II	No	638.26	Yes
68	45	M	II	11.7	Yes	IV	Yes	416.25	Yes
69	36	M	I	5.7	Yes	IV	No	95.22	No
70	47	M	III	8.8	No	III	Yes	38.63	No
71	70	F	III	8.1	Yes	IV	Yes	19.93	Yes
72	83	M	III	2.6	No	I	No	6.38	Yes
73	77	M	III	3.3	No	II	Yes	39.41	Yes
74	44	M	III	4.8	Yes	IV	Yes	122.45	Yes
75	51	F	II	12.9	Yes	IV	Yes	162.25	No
76	61	M	III	4.1	No	II	Yes	411.27	No
77	49	F	I	7.4	Yes	IV	Yes	415.38	Yes
78	41	F	II	3.6	Yes	IV	No	188.35	Yes
79	47	M	II	3.4	No	III	No	3.79	Yes
80	77	F	IV	5	No	I	No	11.07	Yes
81	45	M	III	10.9	Yes	IV	No	1042.32	Yes
82	87	F	IV	6.4	Yes	IV	No	9.4	No
83	44	M	II	1.6	No	I	No	9.68	No
84	41	M	IV	8.8	Yes	IV	Yes	661.2	Yes
85	55	M	IV	7.9	Yes	IV	Yes	18.64	Yes
86	43	M	I	6.8	No	III	Yes	344.84	No

glycolysis by increasing the activity of AKT and mTOR. Consistent with this prediction, miR-873 overexpression in HCC cells was sufficient to induce AKT-S473 and -S6K phosphorylation

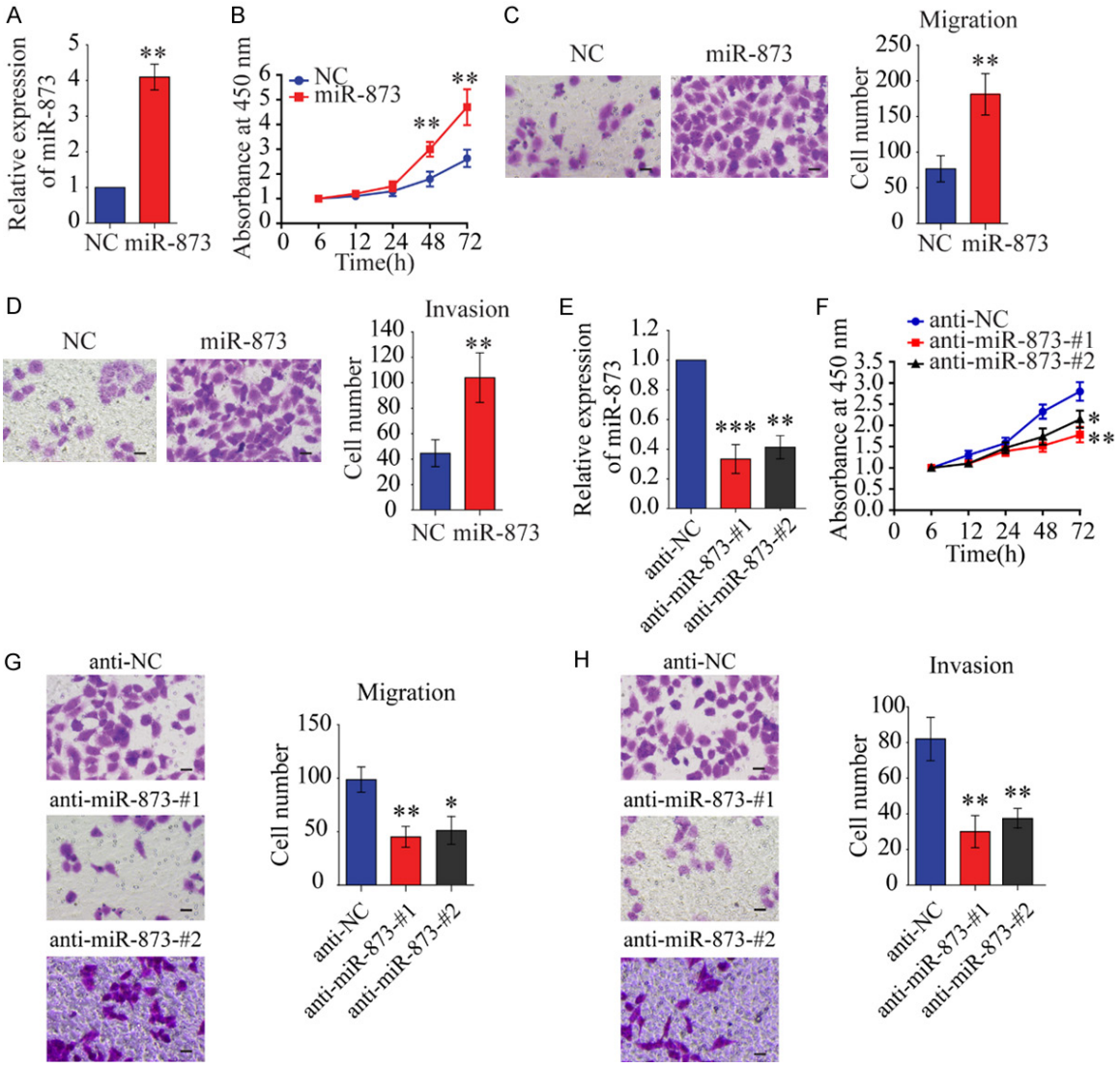

Figure 2. MiR-873 promotes the proliferation, migration, and invasion of liver cancer cells. A. Confirming miR-873 overexpression by qRT-PCR in SMMC-7721 cells transfected with miR-873 mimics. Western blots also were shown. B. The CCK-8 assay was performed to evaluate the effects of miR-873 mimics on cell proliferation in SMMC-7721 cells. C. Transwell-migration assay in SMMC-7721 cells transfected with miR-873 mimics or its control. D. Invasion assay was performed in SMMC-7721 cells treated as indicated. E. Confirming miR-873 inhibition by qRT-PCR in Hep3B cells transfected with miR-873 inhibitors. F. The CCK-8 assay was performed to evaluate the effects of miR-873 inhibitors on cell proliferation in Hep3B cells. G. Migration assay was performed in indicated cells. H. Invasion assay. $^{**}P < 0.01$. C-H. Scale bars, 20 μm.

without affecting the total level of AKT (**Figure 6A**). These data suggest that increased miR-873 expression is associated with an increase in AKT-S473 and -S6K phosphorylation. To examine whether AKT activity might account for the metabolic shift induced by miR-873, we treated miR-873-overexpressing cells with LY294002, a cell-permeable specific inhibitor of phosphatidylinositol 3-kinase. Western blot analysis showed that LY294002 significantly inhibited AKT phosphorylation and decreased the miR-873-induced expression of Glut1 and HK2 (**Figure 6B**). Our results suggest that the inhibition of AKT activity in miR-873-overexpressing cells is sufficient to decrease HCC-induced alterations in the rate of glycolysis. Furthermore, both rapamycin, which represses the activity of mTOR, and LY294002 inhibited the increased rate of glucose and lactate production observed in miR-873-overexpressing

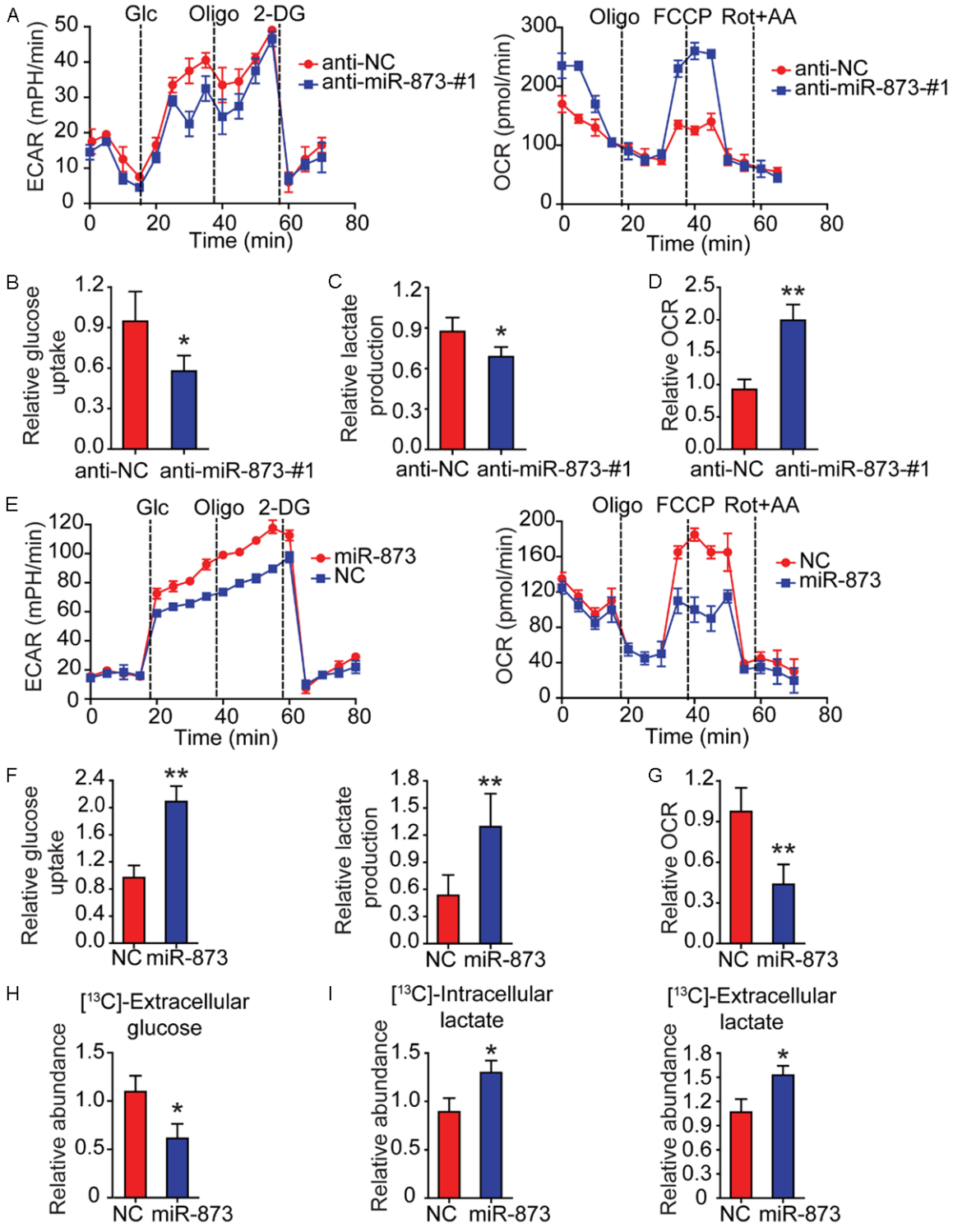

Figure 3. MiR-873 enhances glycolysis in HCC cells. (A) By using a Seahorse Bioscience XFp analyzer, ECAR and OCR of Hep3B cells stably expressing anti-miR-873-#1 or anti-NC were measured. (B) Using the glucose assay kit, cellular glucose uptake was measured in Hep3B cells stably expressing anti-miR-873-#1 or anti-NC. The data were normalized to protein concentrations. (C) By using lactate assay kit, extracellular lactate production was measured in Hep3B cells stably expressing anti-miR-873-#1 or anti-NC. The above data were normalized to protein concentrations. (D) Equal numbers of Hep3B cells stably expressing anti-miR-873-#1 or anti-NC were subjected to an Oxytherm unit to measure the O_2 consumption rate. (E) ECAR and OCR of SMMC-7721 cells with stable overexpression of miR-873 were detected using a Seahorse Bioscience XFp analyzer. (F) Cellular glucose uptake and extracellular lactate production were measured in SMMC-7721 cells with stable overexpression of miR-873 or NC using the glu-

cose or lactate assay kit. The results were normalized to protein concentration. (G) Equal numbers of SMMC-7721 cells with stable overexpression of miR-873 or NC were subjected to an Oxytherm unit to measure their OCRs. (H, I) SMMC-7721 cells with stable overexpression of miR-873 or NC were cultured in medium containing ^{13}C-labeled glucose for the indicated time. Extracellular ^{13}C-labeled glucose (H), intracellular and extracellular ^{13}C-lactate (I) were measured by GC-MS. *P < 0.05 and **P < 0.01.

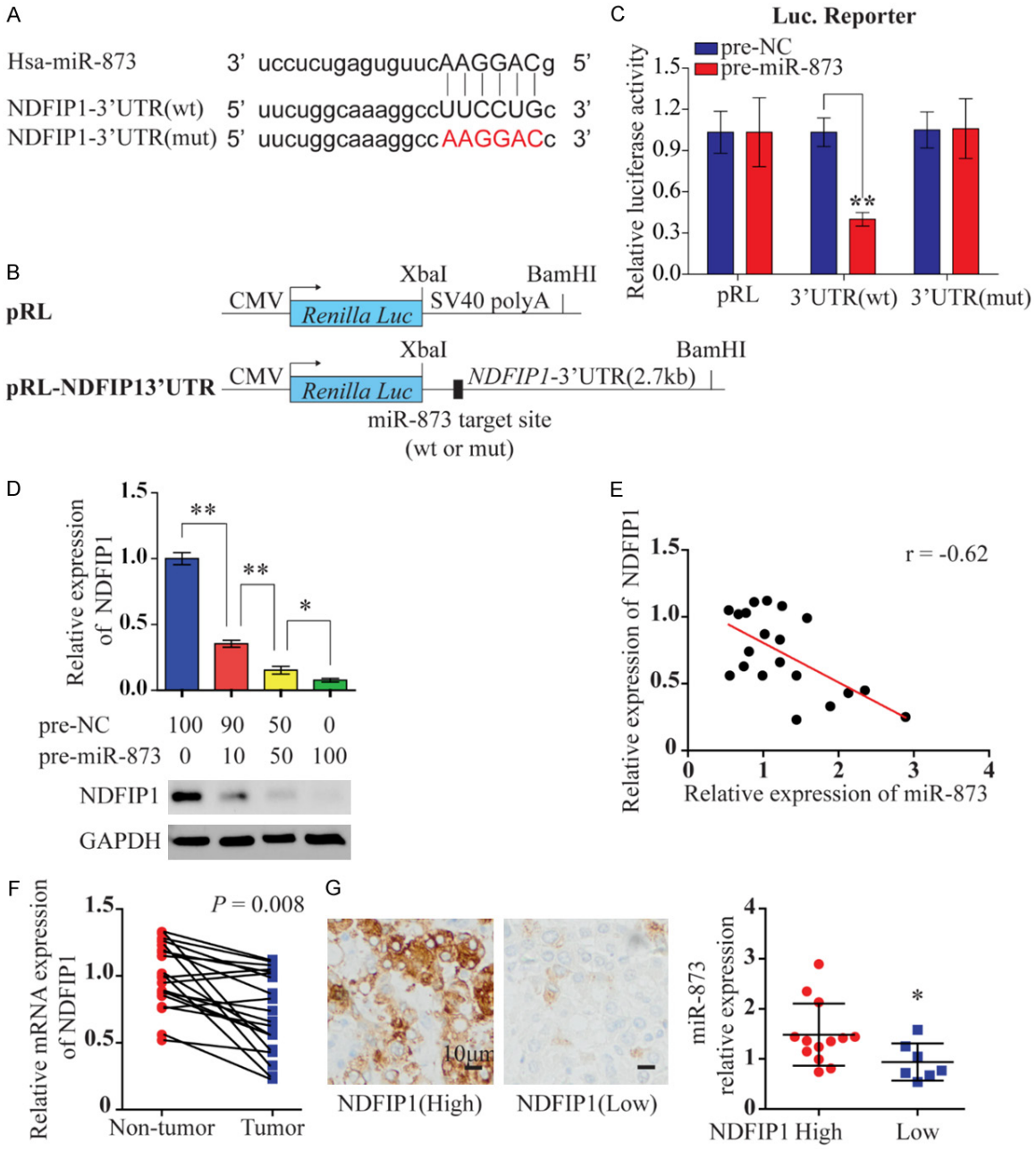

Figure 4. MiR-873 inhibits NDFIP1 expression by targeting its 3'-UTR. A. Mature miR-873 sequences and recognition sites within 3'-UTR of NDFIP1. The seed sequence of miR-873 is shown. WT and mutant NDFIP1-3'-UTR targets are also shown. B. Constructs of *Renilla* luciferase [Luc; (pRL)-CMV] containing WT or mutant NDFIP1 3'-UTR. C. Luciferase activity of pRL and modified constructs containing WT or mutant 3'-UTR. Luciferase constructs were co-transfected with pre-miR-Control (50 nM) or pre-miR-873 (50 nM) into HEK293T cells. *Renilla* luciferase activity was measured and normalized to *firefly* luciferase. D. Immunoblot of endogenous NDFIP1 expression in HEK293T cells 4 days after transfection of increasing amounts of pre-miR-873. E. The correlation between miR-873 and NDFIP1 mRNA expression in 20 human HCC samples using quantitative PCR. F. Spearman's correlation was analyzed. qRT-PCR data of NDFIP1 expression in 20 paired HCC and adjacent non-tumor tissues. G. Representative IHC relationship between NDFIP1 protein expression and miR-873 are shown. Scale bar 10 μm. *P < 0.05 and **P < 0.01.

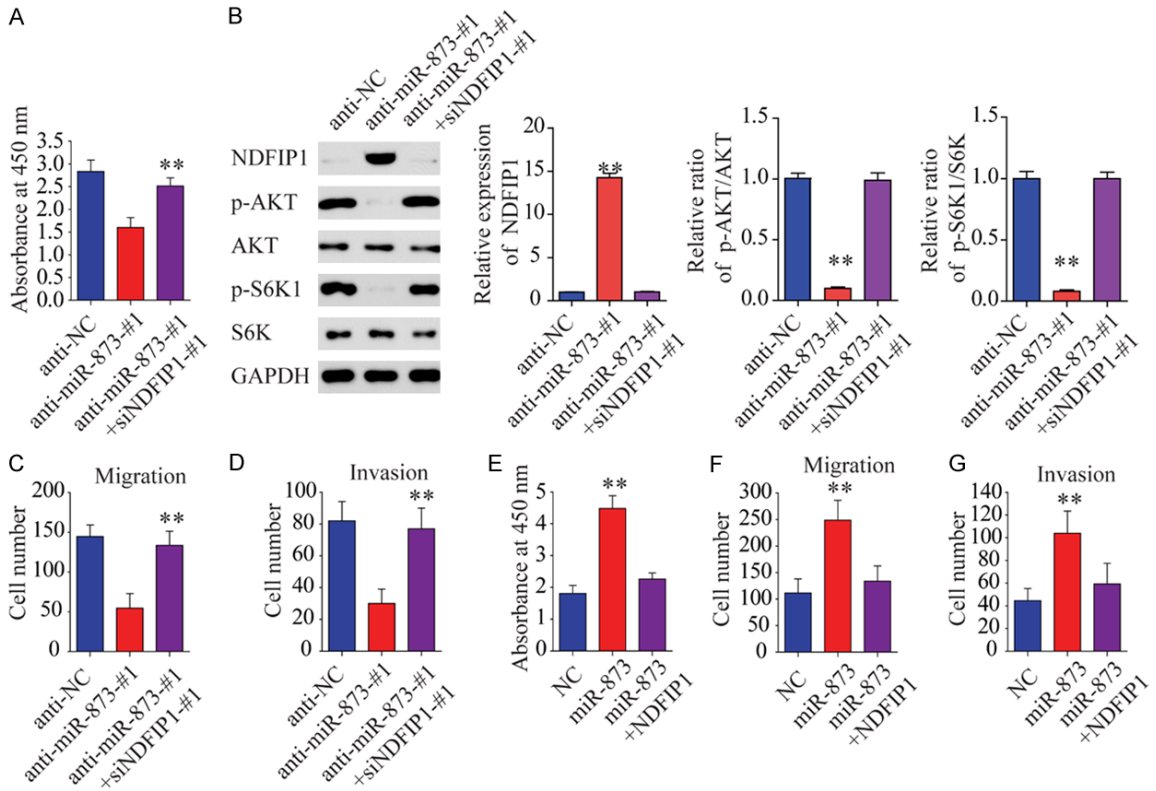

Figure 5. MiR-873 promotes the proliferation, migration, and invasion of liver cancer cells via NDFIP1. (A) The CCK-8 assay was performed to examine the effects of miR-873 inhibitor and siNDFIP1 on cell proliferation in Hep3B cells. (B) Western blot assays show that inhibition of miR-873 decreases AKT and S6K phosphorylation. (C) Transwell-migration assay. (D) Invasion assay was performed. (E) The CCK-8 assay was performed to examine the roles of miR-873 mimics and NDFIP1 in cell proliferation in SMMC-7721 cells. (F) Migration assay and (G) invasion assay was performed in SMMC-7721 cells treated as indicated. $^{**}P < 0.01$.

cells (**Figure 6C** and **6D**). These data suggest that AKT or mTOR activity is required for miR-873-induced changes in glycolysis.

HIF1α drastically upregulates miR-873 expression in HCC cells

Finally, we sought to investigate the mechanism by which miR-873 expression is upregulated in HCC. Since HIF1α can regulate miRNA levels at the transcriptional level and plays a critical role in HCC cell glycolysis [8], we used qRT-PCR to explore the change of miR-873 expression in HCC cells under hypoxic conditions. It was observed that $CoCl_2$ and dimethyloxalylglycine (DMOG) treatment [16] drastically upregulated miR-873 expression (**Figure 7A**). However, HIF1α siRNA decreased miR-873 expression in HCC cells (**Figure 7B**). To further investigate the regulation of miR-873 by HIF1α, the miRStart database (http://mirstart.mbc.nctu.edu.tw/home.php) was used to predict the transcription start site (TSS) of miR-873. The JASPAR database (http://jaspar.genereg.net) was used to predict conserved HIF1α binding elements, also called hypoxia response elements (HREs), in the promoter region of miR-873. It was observed that HIF1α bound to HREs in the 1-kb sequence located upstream of the TSS of miR-873. Thus, we cloned the promoter region of miR-873 (-1 kb) containing the predicted HRE sequences into the pGL3 vector. As expected, treatment of HEK293T cells with $CoCl_2$ increased the luciferase activity of the miR-873 promoter, while small interfering RNA targeting HIF1α (Si-HIF1α) markedly decreased this increase in luciferase activity (**Figure 7C**).

BAY 87-2243, a specific inhibitor of HIF1α [17], was used *in vivo* to treat HCC cell line Hep3B-xenografted male BALB/c nude mice for 15 days. qRT-PCR analysis indicated that BAY 87-2243 reduced miR-873 expression in HCC tissues (**Figure 7D**). Immunohistochemical staining also confirmed the decrease of HIF1α expression in BAY 87-2243-treated HCC tis-

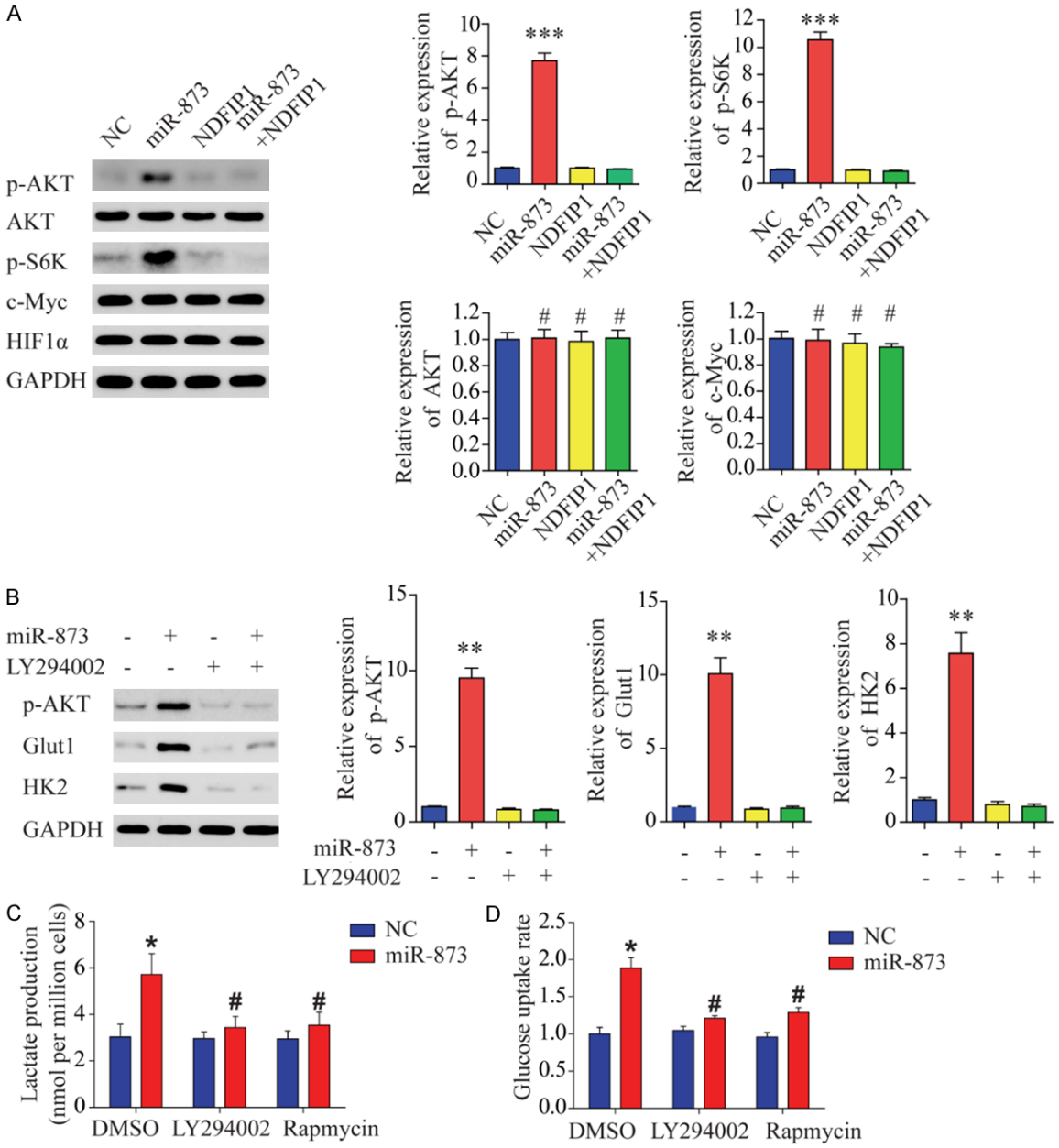

Figure 6. Phosphorylated AKT is required for the miR-873-induced metabolic shift. A. Western blot assays show that miR-873 increases AKT and S6K phosphorylation but does not affect total AKT, c-Myc, or HIF1α expression. B. Western blot assays show that block of AKT phosphorylation with LY294002 blocks miR-873-induced upregulation of HK2 and Glut1 in SMMC-7721 cells. C. Block of AKT phosphorylation with LY294002 decreases miR-873-induced increases in lactate secretion in SMMC-7721 cells. D. Block of AKT phosphorylation with LY294002 decreases miR-873-induced increases in the rate of glucose uptake in SMMC-7721 cells. $*P < 0.05$ and $**P < 0.01$, #represents not statistically significant.

sues compared to the control group (**Figure 7D**).

Discussion

Even though considerable progress has been made in understanding the mechanisms and functional significance of the Warburg effect, the potential impact of miRNAs on HCC cell metabolism still needs further exploration. In this regard, the present study revealed an unexpected role for miR-873 in promoting aerobic glycolysis in HCC cells. Importantly, we identified NDFIP1 as a direct target of miR-873, and

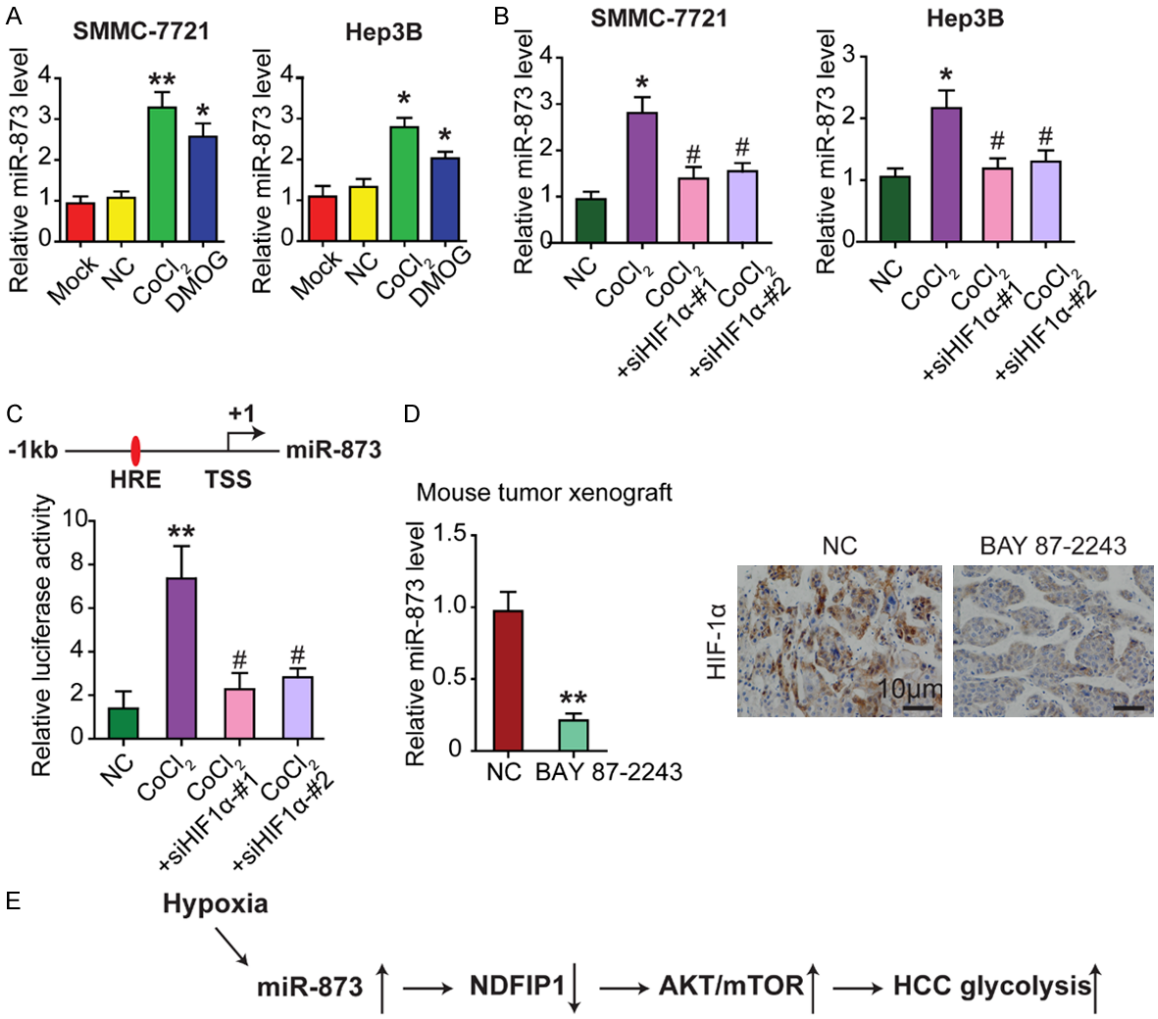

Figure 7. HIF1α drastically upregulates miR-873 expression in HCC cells. A. qRT-PCR was conducted to examine the change of miR-873 expression in HCC cells after being treated with $CoCl_2$ or DMOG for 24 h. B. Treatment of $CoCl_2$ enhances the levels of endogenous miR-873 while silencing HIF1α significantly decreases the expression of miR-873 in HCC cells. C. $CoCl_2$ treatment increases the luciferase activity of the miR-873 promoter in HEK293T cells while Si-HIF1α decreases the increased luciferase activity. TSS and HRE elements in the promoter of miR-873 were shown. D. BAY 87-2243, a HIF1α specific inhibitor, was used to treat Hep3B xenograft male BALB/c-nude mice (4 weeks old) for 15 days. qRT-PCR shows that BAY 87-2243 reduces the expression of miR-873 in HCC cancer tissues. IHC staining confirms that the expression of HIF1α decreases in BAY 87-2243 treated cancer tissues compared to control group. Totally 3 times of independent experiments were repeated. E. Schematic model of miR-873/NDFIP1 axis on HCC growth and metastasis through AKT/mTOR regulation. *$P < 0.05$ and **$P < 0.01$, #represents not statistically significant.

the induction of the metabolic shift by miR-873 was dependent on the NDFIP1/AKT/mTOR axis. We also found that miR-873 expression was negatively related to NDFIP1 levels in patients with HCC. Moreover, we found that miR-873 expression was regulated by HIF1α, thus forming a positive feedback loop to enhance glycolysis in HCC cells. Taken together, these findings support a key role for miR-873 in the development of HCC by enhancing glycolysis, which is potentially significant for designing new therapeutic strategies for cancer.

There is growing evidence that miRNAs play critical roles in the regulation of cellular metabolism. Recent findings indicate that a few miRNAs, such as miR-23a, miR-34a, miR-122, and miR-155, take part in gluconeogenesis, the pentose phosphate pathway, and glycolysis [10, 18, 19]. In our present study, we report that miR-873 is an important novel miRNA linked to HCC cell metabolism. Furthermore, our study confirms that miR-873 promotes glycolysis and lactate production in HCC cells. Although previous studies reported that miR-

873 is downregulated in glioblastoma, breast cancer, and colorectal cancer, and acts as a tumor suppressor [17, 20], our results demonstrated that miR-873 expression was negatively associated with the overall survival of HCC patients. Our finding is consistent with previous studies indicating that miRNAs might function as either oncogenes or tumor suppressors in various cancers, depending on which gene or pathway they regulate [8]. Furthermore, our clinical data support the hypothesis that miR-873 is an independent prognostic indicator for HCC patients, suggesting the significant relevance of miR-873-mediated aerobic glycolysis in the development of human HCC. Indeed, by revealing an unexpected role for miR-873 as a critical regulator of aerobic glycolysis required for HCC cell survival and growth, our results add to our understanding of the mechanisms of aerobic glycolysis. Our findings also provide an additional link between cell metabolism and the progression of HCC. The novel observations from the present study, together with the significant discoveries from previous studies that miR-873 regulates cell cycle, inflammation, and cancer drug resistance [21], place miR-873 at the crossroad of cellular metabolism and tumorigenesis. Thus, miR-873 could be used as a potential biomarker to classify a subtype of HCC patients who have a higher risk of death. Therefore, miR-873 might receive more frequent monitoring and be part of an effective adjuvant treatment. Further studies along this line will likely lead to a potential new therapeutic strategy for cancer.

The underlying mechanism for the altered metabolism of HCC cells might be complicated due to the multiple genes and pathways involved. Of note, NDFIP1, AKT, and S6K1 are reported to be involved in glycolysis [22]. As miRNAs often exert their functions via multiple target genes, in the present study, we focused on the potential role of the miR-873/NDFIP1 axis in the metabolic changes of HCC cells. NDFIP1 is a small endosomal PY-motif-containing membrane protein. It is a potent activator of Nedd4 family members through multiple interactions with the WW domains and also functions as an adaptor protein that brings E3 ligases not only to endosomes but also directly to their substrates [22]. Recently, NDFIP1 was shown to regulate the PTEN/AKT signaling pathway [15], suggesting that NDFIP1 might affect glycolysis in HCC cells. Our data demonstrated that NDFIP1 is a direct target of miR-873. Most importantly, we discovered that the inhibition of the Warburg effect by miR-873 is dependent on the NDFIP1/AKT/mTOR axis, as overexpression of NDFIP1 or treatment with an AKT/mTOR inhibitor abated the effects of miR-873 on aerobic glycolysis. As NDFIP1 is a regulator of glycolysis [22], we also demonstrated that the expression of glycolysis-related genes, including GLUT1, HK2, AKT, and S6K, was affected by NDFIP1 and miR-873, suggesting that miR-873 is linked to metabolic control through its downstream regulation of NDFIP1. Our study identifies NDFIP1 as a key mediator of the metabolic effects triggered by miR-873 in HCC. Thus, our data establish the physiological and pathological significance of miR-873 in regulating the NDFIP1/AKT/mTOR-mediated Warburg effect. An inhibitor of miR-873 may be useful for the treatment of HCC patients with low NDFIP1 expression.

Hypoxia in the microenvironment is one of the most common features of solid tumors [2]. HCC cells adjust their transcription and translation to maintain cellular homeostasis and enable adaptive survival under hypoxic stress conditions. Some miRNAs are regulated by hypoxia and are thus termed hypoxia-responsive miRNAs. Consistent with previous studies, we found the upregulation of miR-873 expression in HCC cells subjected to hypoxia or in a hypoxic environment induced by the use of $CoCl_2$. Moreover, we found that miR-873 is a HIF1α-responsive miRNA and the ectopic expression of HIF1α can greatly increase miR-873 expression. The upregulation of miR-873 can, in turn, lead to the further upregulation of glycolysis-related genes, thus forming a positive feedback loop. This positive feedback reinforces the critical role of miR-873/NDFIP1 in mediating the Warburg effect and tumor progression in HCC.

Acknowledgements

This work was supported by grants by the National Natural Science Foundation of China (31571241, 31660266).

Disclosure of conflict of interest

None.

Address correspondence to: Feng Liu, Department of Nephrology, China-Japan Union Hospital of Jilin

University, Changchun, China. E-mail: jdliufeng@163.com; Shunzi Jin, NHC Key Laboratory of Radiobiology, Jilin University, Changchun, China. E-mail: jinsz@jlu.edu.cn

References

[1] Hong X, Song R, Song H, Zheng T, Wang J, Liang Y, Qi S, Lu Z, Song X and Jiang H. PTEN antagonises Tcl1/hnRNPK-mediated G6PD pre-mRNA splicing which contributes to hepatocarcinogenesis. Gut 2014; 63: 1635-47.

[2] Song R, Song H, Liang Y, Yin D, Zhang H, Zheng T, Wang J, Lu Z, Song X and Pei T. Reciprocal activation between ATPase inhibitory factor 1 and NF-κB drives hepatocellular carcinoma angiogenesis and metastasis. Hepatology 2014; 60: 1659-1673.

[3] Qu C, He D, Lu X, Dong L, Zhu Y, Zhao Q, Jiang X, Chang P, Jiang X and Wang L. Salt-inducible Kinase (SIK1) regulates HCC progression and WNT/β-catenin activation. J Hepatol 2016; 64: 1076-1089.

[4] Song H, Pu J, Wang L, Wu L, Xiao J, Liu Q, Chen J, Zhang M, Liu Y and Ni M. ATG16L1 phosphorylation is oppositely regulated by CSNK2/casein kinase 2 and PPP1/protein phosphatase 1 which determines the fate of cardiomyocytes during hypoxia/reoxygenation. Autophagy 2015; 11: 1308-1325.

[5] He D, Huang C, Zhou Q, Liu D, Xiong L, Xiang H, Ma G and Zhang Z. HnRNPK/miR-223/FBXW7 feedback cascade promotes pancreatic cancer cell growth and invasion. Oncotarget 2017; 8: 20165.

[6] He D, Miao H, Xu Y, Xiong L, Wang Y, Xiang H, Zhang H and Zhang Z. MiR-371-5p facilitates pancreatic cancer cell proliferation and decreases patient survival. PLoS One 2014; 9: e112930.

[7] Song K, Kwon H, Han C, Zhang J, Dash S, Lim K and Wu T. Active glycolytic metabolism in CD133(+) hepatocellular cancer stem cells: regulation by MIR-122. Oncotarget 2015; 6: 40822-35.

[8] Zhang H, Guo X, Feng X, Wang T, Hu Z, Que X, Tian Q, Zhu T, Guo G and Huang W. MiRNA-543 promotes osteosarcoma cell proliferation and glycolysis by partially suppressing PRMT9 and stabilizing HIF-1α protein. Oncotarget 2017; 8: 2342-2355.

[9] Klionsky DJ, Abdelmohsen K, Abe A, Abedin MJ, Abeliovich H, Acevedo Arozena A, Adachi H, Adams CM, Adams PD and Adeli K. Guidelines for the use and interpretation of assays for monitoring autophagy. Autophagy 2016; 12: 1-222.

[10] Liu AM, Xu Z, Shek FH, Wong KF, Lee NP, Poon RT, Chen J and Luk JM. miR-122 targets pyruvate kinase M2 and affects metabolism of hepatocellular carcinoma. PLoS One 2014; 9: e86872.

[11] Wang RJ, Li JW, Bao BH, Wu HC, Du ZH, Su JL, Zhang MH, Liang HQ. MicroRNA-873 (miRNA-873) inhibits glioblastoma tumorigenesis and metastasis by suppressing the expression of IGF2BP1. J Biol Chem 2015; 290: 8938-48.

[12] Gao Y, Xue Q, Wang D, Du M, Zhang Y and Gao S. miR-873 induces lung adenocarcinoma cell proliferation and migration by targeting SRCIN1. Am J Transl Res 2015; 7: 2519-26.

[13] Wu DD, Li XS, Meng XN, Yan J, Zong ZH. MicroRNA-873 mediates multidrug resistance in ovarian cancer cells by targeting ABCB1. Tumour Biol 2016; 37: 10499-506.

[14] Zhang Y, Yang L, Ling C and Heng W. HuR facilitates cancer stemness of lung cancer cells via regulating miR-873/CDK3 and miR-125a-3p/CDK3 axis. Biotechnol Lett 2018; 40: 623-631.

[15] Howitt J, Low LH, Putz U, Doan A, Lackovic J, Goh CP, Gunnersen J, Silke J, Tan SS. Ndfip1 represses cell proliferation by controlling Pten localization and signaling specificity. J Mol Cell Biol 2015; 7: 119-31.

[16] Taheem DK, Foyt DA, Loaiza S, Ferreira SA, Ilic D, Auner HW, Grigoriadis AE, Jell G and Gentleman E. Differential regulation of human bone marrow mesenchymal stromal cell chondrogenesis by hypoxia inducible Factor-1α hydroxylase inhibitors. Stem Cells 2018; 36: 1380-1392.

[17] Ellinghaus P, Heisler I, Unterschemmann K, Haerter M, Beck H, Greschat S, Ehrmann A, Summer H, Flamme I and Oehme F. BAY 87-2243, a highly potent and selective inhibitor of hypoxia-induced gene activation has antitumor activities by inhibition of mitochondrial complex I. Cancer Med 2013; 2: 611-24.

[18] Wang B, Hsu SH, Frankel W, Ghoshal K and Jacob ST. Stat3-mediated activation of microRNA-23a suppresses gluconeogenesis in hepatocellular carcinoma by down-regulating Glucose-6-phosphatase and peroxisome proliferator-activated receptor gamma, coactivator 1 alpha. Hepatology 2012; 56: 186-197.

[19] Kim HR, Roe JS, Lee JE, Cho EJ, Youn HD. p53 regulates glucose metabolism by miR-34a. Biochem Biophys Res Commun 2013; 437: 225-31.

[20] Cui J, Yang Y, Li H, Leng Y, Qian K, Huang Q, Zhang C, Lu Z, Chen J and Sun T. MiR-873 regulates ERα transcriptional activity and tamoxifen resistance via targeting CDK3 in breast cancer cells. Oncogene 2015; 34: 3895-3907.

[21] Liu X, He F, Pang R, Zhao D, Qiu W, Shan K, Zhang J, Lu Y, Li Y and Wang Y. Interleukin-17 (IL-17)-induced microRNA 873 (miR-873) con-

tributes to the pathogenesis of experimental autoimmune encephalomyelitis by targeting A20 ubiquitin-editing enzyme. J Biol Chem 2014; 289: 28971-86.

[22] Mund T and Pelham HR. Regulation of PTEN/Akt and MAP kinase signaling pathways by the ubiquitin ligase activators Ndfip1 and Ndfip2. Proc Natl Acad Sci U S A 2010; 107: 11429-34.

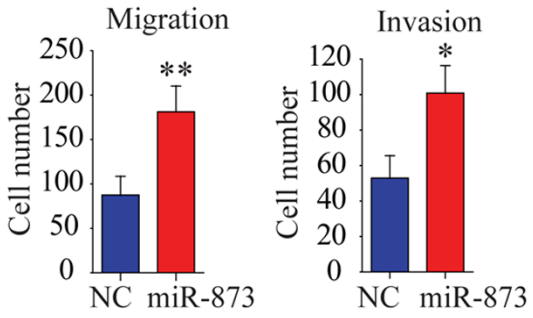

Figure S1. MiR-873 promotes the migration, and invasion of liver cancer cells. SMMC-7721 cells transfected with miR-873 mimics or its control were pre-treated with mitomycin-C (10 μg/ml) and then migration and invasion were analyzed.

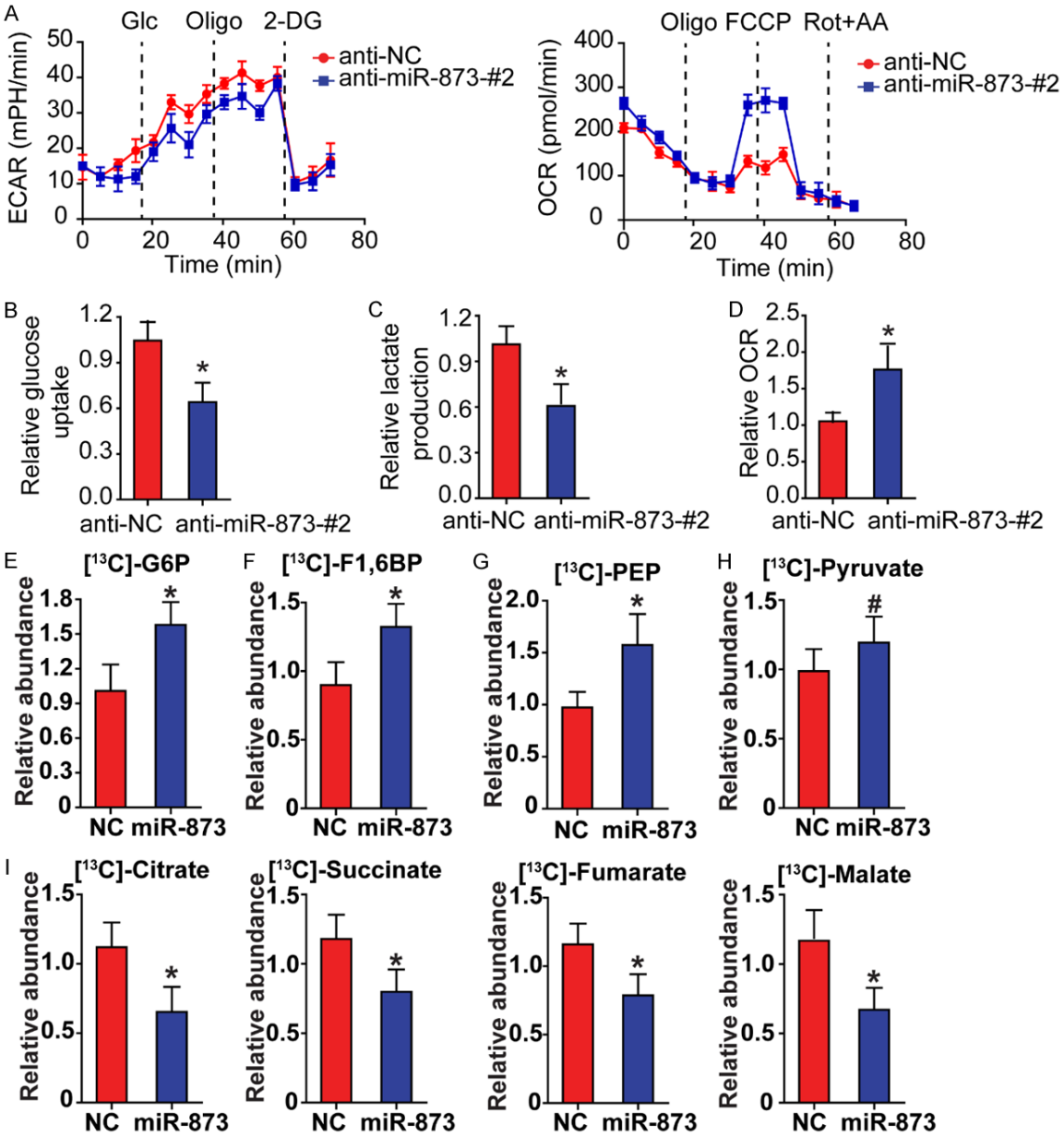

Figure S2. MiR-873 enhances glycolysis in HCC cells (Part II). (A) By using a Seahorse Bioscience XFp analyzer, ECAR and OCR of Hep3B cells stably expressing anti-miR-873-#2 or anti-NC were measured. (B) Using the glucose assay kit, cellular glucose uptake was measured in Hep3B cells stably expressing anti-miR-873-#2 or anti-NC. The data were normalized to protein concentrations. (C) By using lactate assay kit, extracellular lactate production was measured in Hep3B cells stably expressing anti-miR-873-#2 or anti-NC. The above data were normalized to protein concentrations. (D) Equal numbers of Hep3B cells stably expressing anti-miR-873-#2 or anti-NC were subjected to an Oxytherm unit to measure the O_2 consumption rate. SMMC-7721 cells with stable overexpression of miR-873 or NC were cultured in medium containing ^{13}C-labeled glucose for the indicated time. ^{13}C-G6P (E), ^{13}C-F1,6BP (F), ^{13}C-PEP (G), ^{13}C-pyruvate (H), and cellular ^{13}C-labeling TCA cycle metabolites (I) were measured by GC-MS.

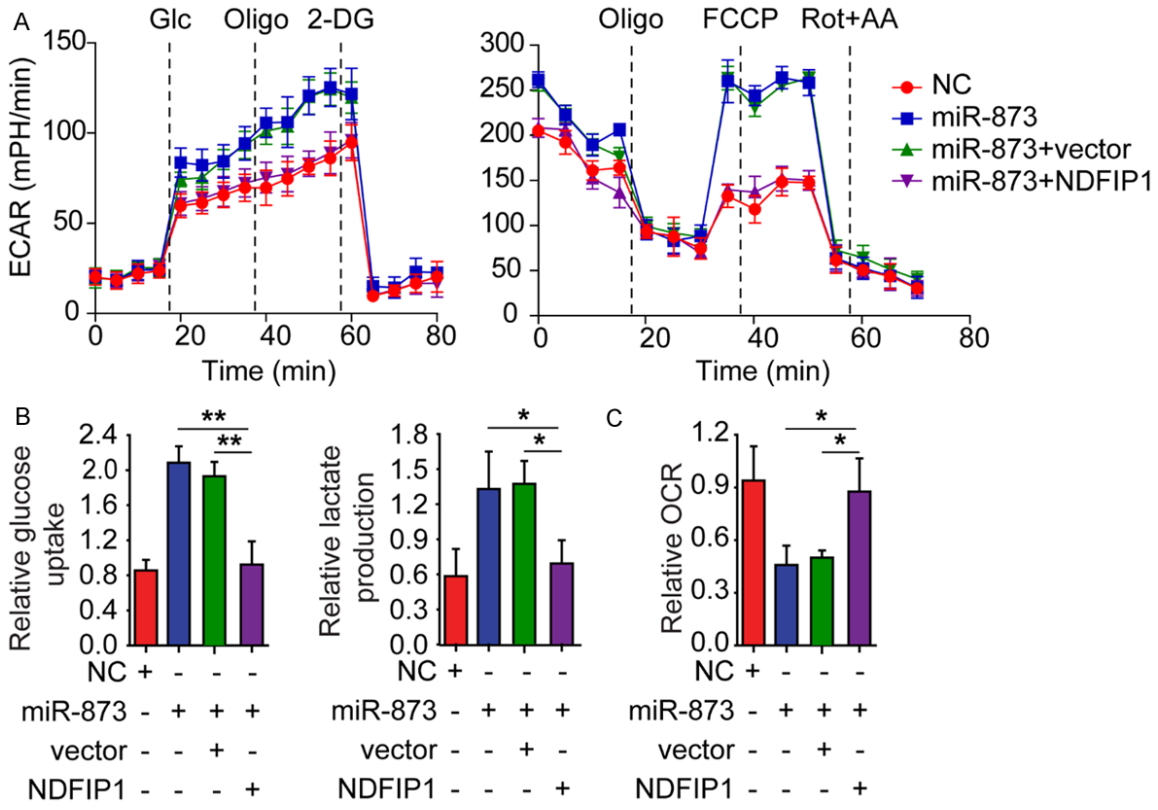

Figure S3. MiR-873 enhances glycolysis in HCC cells via NDFIP1. A. ECAR and OCR of SMMC-7721 cells with miR-873 mimics and NDFIP1 overexpression were detected using a Seahorse Bioscience XFp analyzer. B. Cellular glucose uptake and extracellular lactate production were measured in SMMC-7721 cells with miR-873 mimics and NDFIP1 overexpression using the glucose or lactate assay kit. The results were normalized to protein concentration. C. Equal numbers of SMMC-7721 cells with miR-873 mimics and NDFIP1 overexpression were subjected to an Oxytherm unit to measure their OCRs. $*P < 0.05$ and $**P < 0.01$.

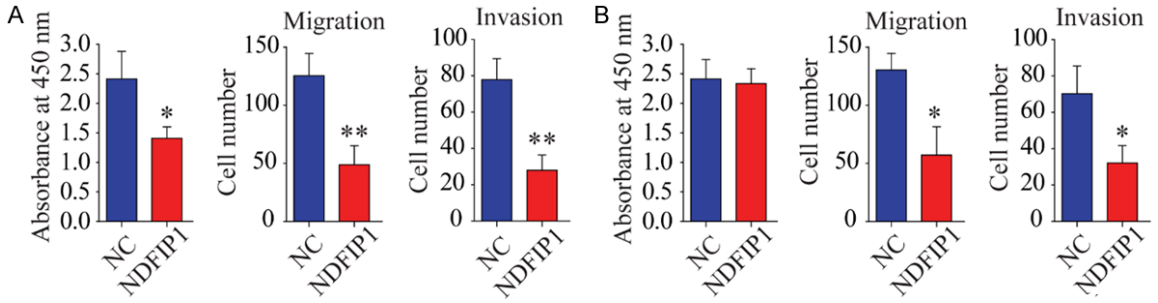

Figure S4. NDFIP1 inhibited the proliferation, migration and invasion of HCC cells. A. SMMC-7721 cells were transfected with NDFIP1 or vector. CCK-8 assay, transwell-migration assay and invasion assay were performed. B. Above assay was conducted under the treatment of Z-VAD.

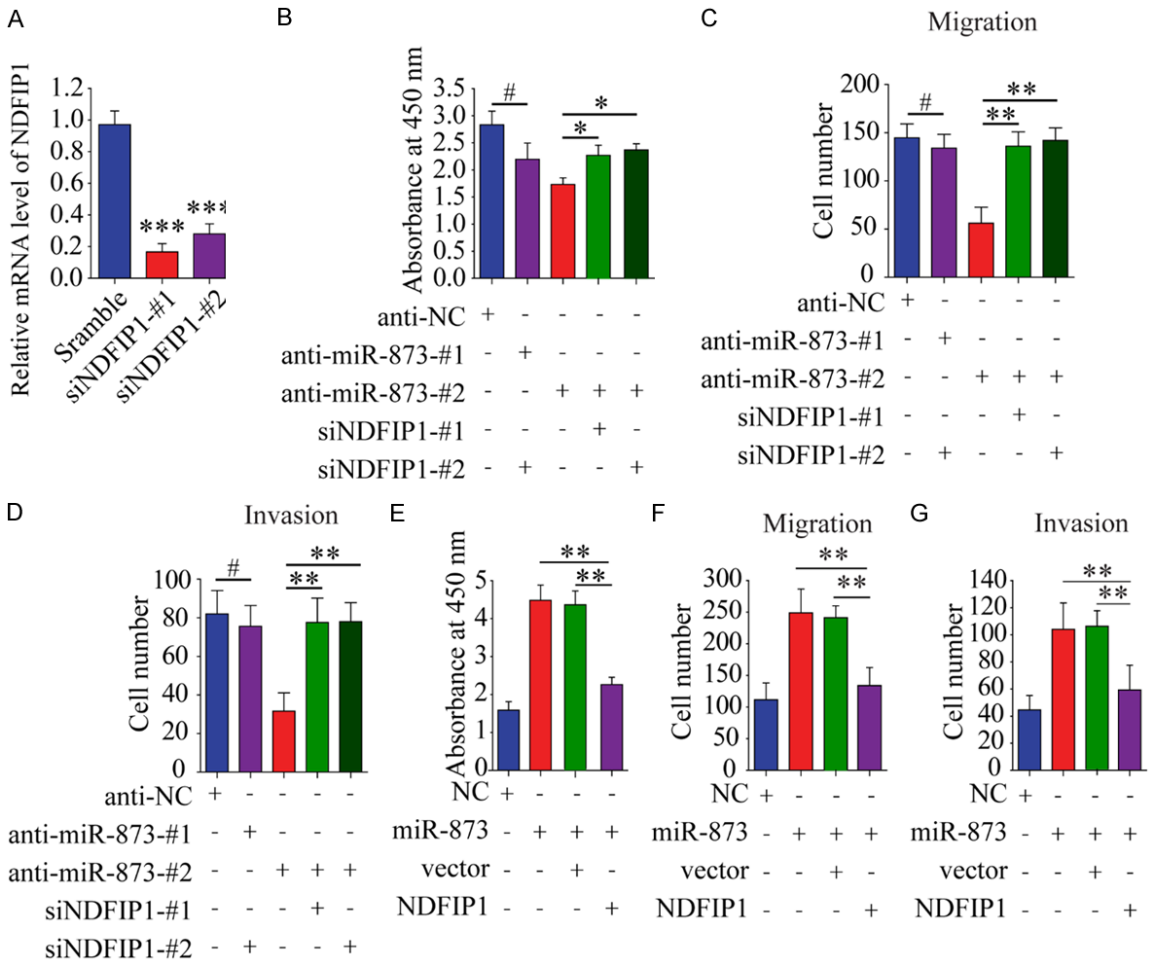

Figure S5. MiR-873 promotes the proliferation, migration, and invasion of liver cancer cells via NDFIP1. (A) Relative expression level of NDFIP1 with 2 specific siRNA. (B) The CCK-8 assay was performed to examine the effects of miR-873 inhibitor and siNDFIP1 on cell proliferation in Hep3B cells. (C) Transwell-migration assay. (D) Invasion assay was performed. (E) The CCK-8 assay was performed to examine the roles of miR-873 mimics and NDFIP1 in cell proliferation in SMMC-7721 cells. (F) Migration assay and (G) invasion assay was performed in SMMC-7721 cells treated as indicated. $^{**}P < 0.01$.